ECS Transactions, 9 (1) 123-132 (2007)
10.1149/1.2766881 ©The Electrochemical Society

Anisotropic Resistivity of PMMA Doped with Gold

F. S. Teixeira[a,b], R. D. Mansano[a], M. C. Salvadori[b], M. Cattani[b] and I. G. Brown[c]

[a] Laboratory of Integrated Systems, Polytechnic School, Av. Prof. Luciano Gualberto Trav. 3-158, University of São Paulo, CEP 05508-900 São Paulo, Brazil
[b] Institute of Physics, University of São Paulo, C.P. 66318, CEP 05315-970 São Paulo, Brazil
[c] Lawrence Berkeley National Laboratory, 1 Cyclotron Road, Berkeley, California 94720

In this work PMMA was deposited on glass substrate, nanolithographed using Atomic Force Microscopy (AFM) and doped with gold using very low energy ion implantation. Samples with different geometries were prepared in order to identify anisotropic resistivity due to an anisotropic surface morphology. One of the samples was fabricated with parallel lines along the substrate length and the second one with parallel lines perpendicular to it. The PMMA with gold implanted presented resistivities in the range 7.7 x 10^{-8} Ω.m to 0.23 Ω.m. For any PMMA surface morphology the resistivity decreased when the gold dose increased. The anisotropic factor for both morphologies described above presented a prominent peak for a dose of 1.15 x 10^{16} atoms/cm^2. Finally, a new sample of PMMA with gold implanted dose of 1.15 x 10^{16} atoms/cm^2 was prepared and an I-V curve was obtained, showing clearly that the material is a semiconductor.

Introduction

The purpose of this work was to describe a new semiconductor material made by PMMA doped with gold using very low energy ion implantation. In addition, nanolithography is performed on the PMMA generating an anisotropic surface morphology, resulting in an anisotropic resistivity.

Recent experiments on the electrical conductivity of very thin metallic films have revealed more precise and detailed features in the transport properties. According to many works (1 – 10) a quantum mechanical theory is necessary for explaining the thin film electrical conductivity when the following conditions are obeyed: (a) $\delta \leq \ell_0$, where δ is the film thickness and ℓ_0 is the electronic mean free path and (b) the energy-level quantization is enhanced in the direction of the film thickness.

In preceding works (11 – 14) we have studied very thin platinum and gold films. These films have been fabricated with isotropic surfaces. According to our analysis quantum size effects (QSE) play a fundamental role in the electrical conductivity for $\delta <$ 4 nm. For thickness larger than 4 nm the QSE begin to decrease, however the conductivity process can be well described by semiclassical models only for films with $\delta \geq$ 10 nm. To explain the electrical resistivities of the platinum and gold films we have proposed a quantum-mechanical approach using the Boltzmann transport equations. A good agreement was found between the theoretical predictions for the resistivity and the experimental results (11 - 14).

In more recent papers (15) our preceding model (11 – 14) was generalized in order to predict the resistivities of films with anisotropic surfaces. More specifically we studied the anisotropic case when the film surfaces have different morphological properties along two orthogonal directions. It was shown that depending on these differences the surface-induced resistivities along these directions can be different. This effect was already experimentally observed (16) for very thin Pt films with thickness in the range $0.90 \leq \delta \leq 11.10$ nm. In that work (16) we have fabricated different morphological properties along two orthogonal directions, generating different resistivities along these directions.

In this work PMMA was deposited on glass substrate, nanolithographed using Atomic Force Microscopy (AFM) and doped with gold using very low energy ion implantation. Samples with different geometries were prepared in order to identify anisotropic resistivity due to an anisotropic surface morphology.

Experimental Procedure

Glass microscope slides, with surface RMS roughness of about 0.5 nm, were cut into 14 mm by 5 mm pieces, cleaned and baked at 150°C for 10 minutes to remove residual humidity, and PMMA then deposited on the samples using a spin coater. The samples were then baked again at 180°C for 20 minutes to evaporate the polymer solvent. We used PMMA ARP671.06, with molecular weight 950 K and concentration of 6% in clorobenzene, from Allresist. The average PMMA film thickness was 500 nm and its typical RMS roughness < 0.5 nm.

A selected area of the PMMA was electron beam scanned in a Scanning Electron Microscope (JEOL model JSM-6460 LV) using an e-beam nanolithography system (Nanometer Pattern Generation System - NPGS). The purpose was to delimitate a small area of PMMA of 20 x 20 μm^2 to be nanolithographed by AFM as illustrated in Figure 1. The e-beam lithography was performed with a 30 kV, 50 pA electron beam. The applied electron dose was 225 $\mu C/cm^2$ with an exposure time of 362 μs at each scan point. The samples were then immersed in a developing solution of 1 MIBK (methyl isobutyl ketone) : 3 IPA (isopropyl alcohol) for 2 minutes and rinsed in IPA for 30 seconds.

The nanolithography was performed by AFM and the equipment used was a NanoScope IIIa with a tapping mode probe. Our procedure was to first obtain a tapping mode image of a selected region, then to perform contact nanolithography, and finally to obtain a new tapping mode image to visualize the modified surface. The lithography mechanism is similar to image acquisition, but with the scanning tip maintained in constant contact with the surface so as to scribe each scan line, generating a pattern of parallel lines on the PMMA surface. To perform the lithography it is necessary to apply a higher force, between tip and surface, than that used for image acquisitions. For the lithography performed here, the force applied was about 0.9 μN. Two different samples were prepared lithographing a region with 20 x 20 μm^2 at the center of the samples (see Figure 1). One of the samples was fabricated with parallel lines along the substrate length and the second one with parallel lines perpendicular to it. Note that, during image acquisition, the tip touches the surface only gently and the polymer is not modified.

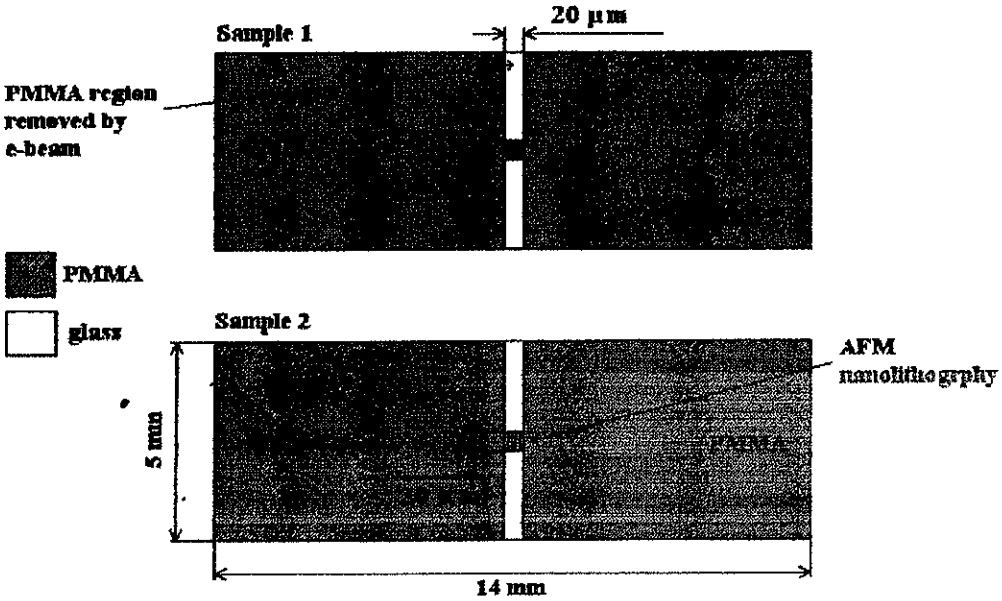

Figure 1. PMMA samples lithographed by electron beam in a Scanning Electron Microscope. The small area of 20 x 20 μm^2 is the region to be nanolithographed by AFM. The scheme is out of scale.

Electrical contacts were formed at the both ends of the substrates using silver glue followed by plasma deposition of relatively thick (180 nm) gold films onto the contacts, with a mask protecting the center of the samples, as shown in Figure 2.

Three samples were then positioned in the plasma deposition vacuum chamber. Two of them with lines lithographed as described above and one with no lithography. The samples resistances were measured throughout the gold ion implantation process. The resistance was measured after the first six pulses and subsequently after every three pulses, thus determining the material resistance as a function of gold implantation without removing the sample from vacuum for each individual measurement.

The very low energy ion implantation was performed using a filtered vacuum arc plasma deposition method that has been fully described elsewhere (17). Briefly, a repetitively-pulsed vacuum arc plasma gun equipped with a gold cathode was used to form a dense metal (Au) plasma, which is then transported through a 90° bent solenoidal magnetic field to remove any solid particulates (cathode debris) from the plasma stream. The plasma is then allowed to arrive on the substrate that is positioned near the exit of the solenoid filter. For the work described here the plasma pulses were 5 ms long and the repetition rate was 1 pulse/sec. Importantly, we note that the vacuum arc plasma deposition method that we have used is an energetic deposition, with the Au ion flux having a directed ion energy of 49 eV (18, 19), resulting in ion implantation in PMMA, as confirmed by simulation using the Stopping Range of Ions in Matter (SRIM) program (20).

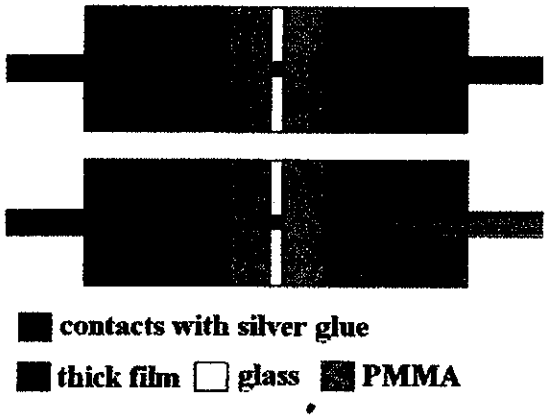

Figure 2. Scheme showing the electrical contacts at both ends of the substrates using silver glue and thick gold films onto the contacts.

The dose of gold implanted was determined from the number of plasma pulses using a prior calibration. A gold film was deposited on silicon wafer as substrate with an ink mark that was removed after the deposition to form a step in the film whose thickness could be accurately determined by AFM. Considering that the deposition method produces film void free and fully dense (21), the number of gold atoms deposited by pulse can be determined using the known gold density.

Results and Discussion

The resistivities, ρ_1 (sample with lithographed lines in the direction of the substrate length) and ρ_2 (sample with lithographed lines along the perpendicular direction of the substrate length), were determined from the respective measured resistances R_1 and R_2. Considering that the sample with no lithography had the same dimensions of the lithographed samples and that the lithographed regions were squares (as described above they were 20 x 20 μm^2), then the resistivities of the lithographed regions cold be determined by $\rho_1 = (R_1 - R_3)d$ and $\rho_2 = (R_2 - R_3)d$, where R_3 is the resistance of the sample with no lithography and d is the average depth of the gold implantation. The parameter d, calculated using the SRIM program, was found to be $d = 2.7$ nm.

The PMMA with gold implanted presented resistivities in the range 7.7 x 10^{-8} Ω.m to 0.23 Ω.m. The resistivities measured for both lithographed samples as function of the dose of gold implanted are shown in the graphs of Figure 3. The resistivity for both cases decreases when the dose increases as it is expected.

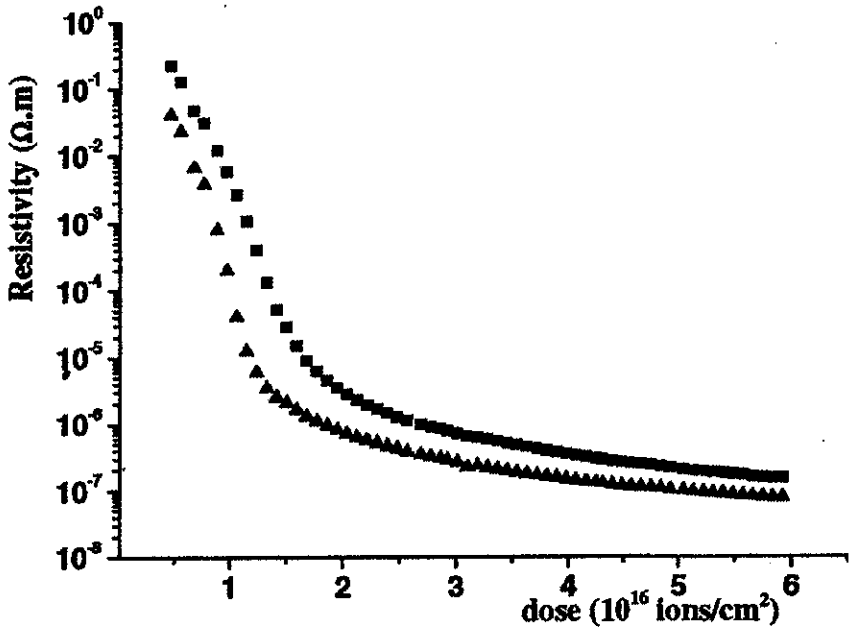

Figure 3. Resistivities measured for both lithographed samples as function of the dose of gold implanted. The squares represent the resistivity (ρ_1) of the sample with lithographed lines parallel to the direction of the substrate length and the triangles represent the resistivity (ρ_2) of the sample with lithographed lines perpendicular to the direction of the substrate length.

It was expected that the sample with lithographed lines parallel to the direction of the substrate length should have lower resistivity than the sample with lithographed lines parallel to the direction perpendicular to the substrate length. But the result was just the opposite. To interpret this result, let us analyze the lithography process. Initially we will show that the morphological wavelengths (λ) observed by AFM images of the PMMA nanolithographed are not small enough to produce the resistivity anisotropic effect. Following we will suggest a possible justification for the observed resistivity anisotropy.

A typical AFM image of a nanolithographed region of PMMA is shown in Figure 4, where 512 lines were scribed in a 20 μm square. Using the Power Spectral Density (PSD) analysis (22) we verified that the morphological surface wavelengths (λ) were found to be 78.0 nm, 39.2 nm and 19.4 nm. The quantum theory predicts (15,16) that the anisotropic resistivity is essentially due to conduction electrons with de Broglie wavelength $\lambda_c \approx \lambda$. Since for semiconductors $\lambda_c \sim 1.2$ nm and that for our samples the condition $\lambda >> \lambda_c$ is obeyed, a negligible anisotropic effect is expected.

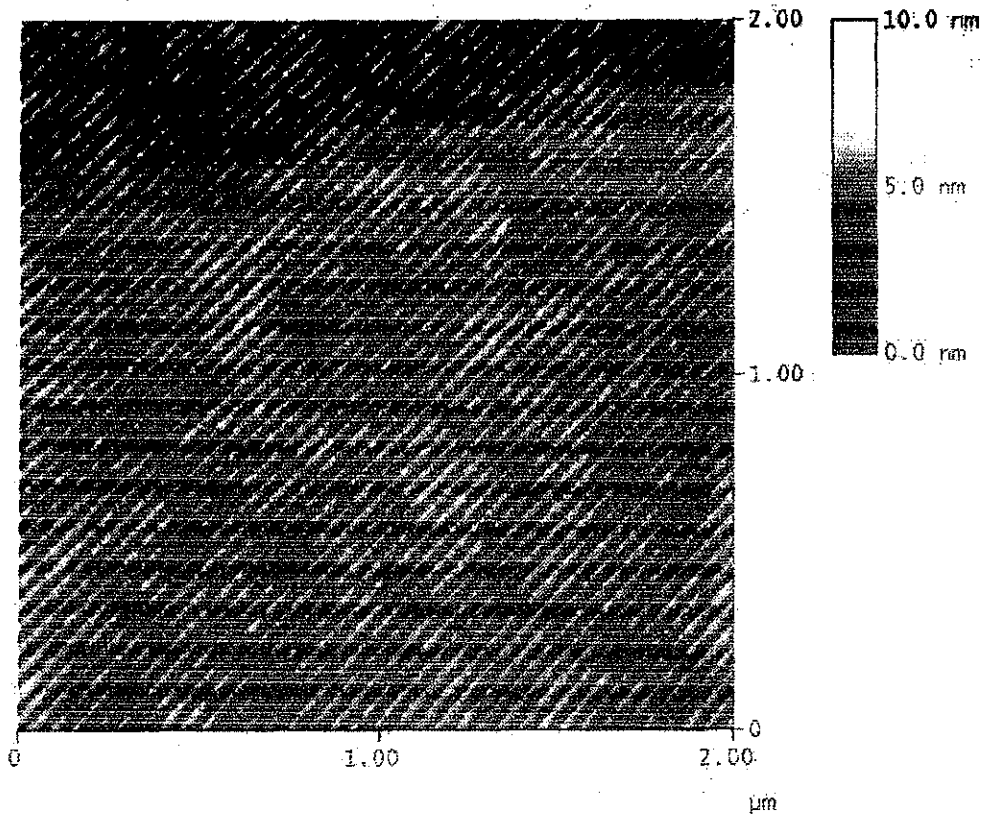

Figure 4. AFM image of a nanolithographed region on PMMA surface. The scan was 20 µm and contained 512 lines.

Now considering an AFM higher magnification of a nanolithographed region as presented in Figure 5, it is possible to observe a fine structure, where small nodules can be seen between the scribed lines. This nodular morphology has already been observed in the developed PMMA (23, 24) and, in our case, they are aligned during the AFM lithography process. In addition, we can also find in the literature that PMMA has a local order with average main-chain distance subnanometric (25 - 28). With this in mind, we can interpret that each nodule has an internal structure with subnanometric periodicity and, aligning these nodules, we can reach a preferential orientation of the main-chains. This interpretation can justify the lower sample resistivity for the lithographed lines along the perpendicular direction of the substrate length.

Figure 6 presents the anisotropic factor ρ_1/ρ_2 as function of the implantation gold dose. A prominent peak is observed for a dose of 1.15 x 10^{16} atoms/cm^2. With high doses (> 2 x 10^{16} atoms/cm^2), the preferential orientation of the main-chains can be progressively destroyed, consequently reducing the anisotropic effect. For lower doses (< 1 x 10^{16} atoms/cm^2) the gold implanted PMMA has not been characterized enough to permit an interpretation of the low anisotropic effect.

Finally, a new sample of PMMA with gold implanted dose of 1.15 x 10^{16} atoms/cm^2 was prepared and an I-V curve was obtained (Figure 7). This curve shows clearly that the material is a semiconductor.

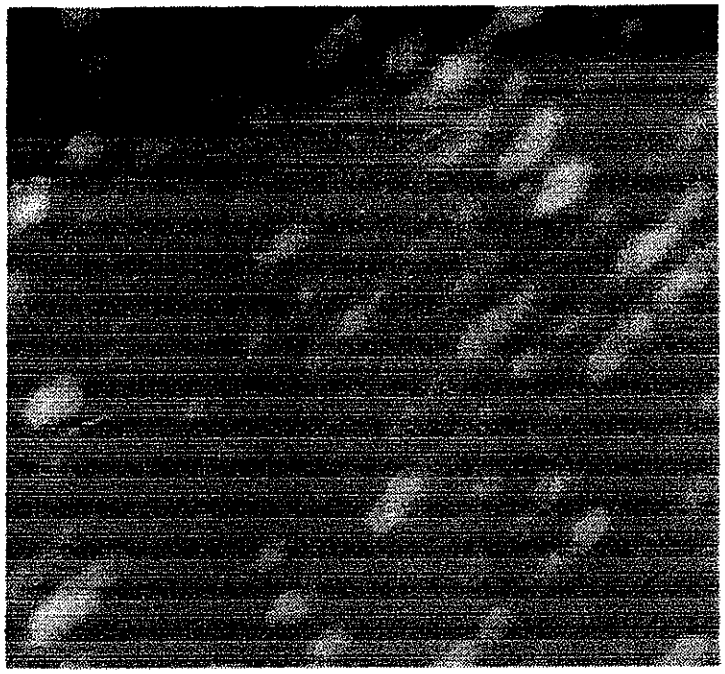

Figure 5. AFM image showing aligned debris in the PMMA furrows. The image width is 500 nm.

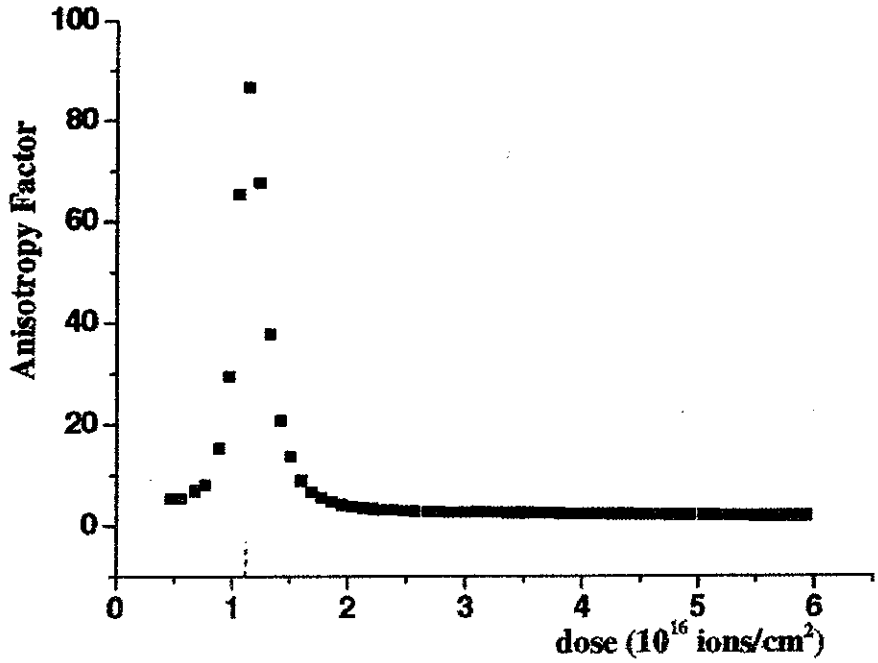

Figure 6. Resistivity anisotropic factor ρ_1/ρ_2 as function of the implantation gold dose.

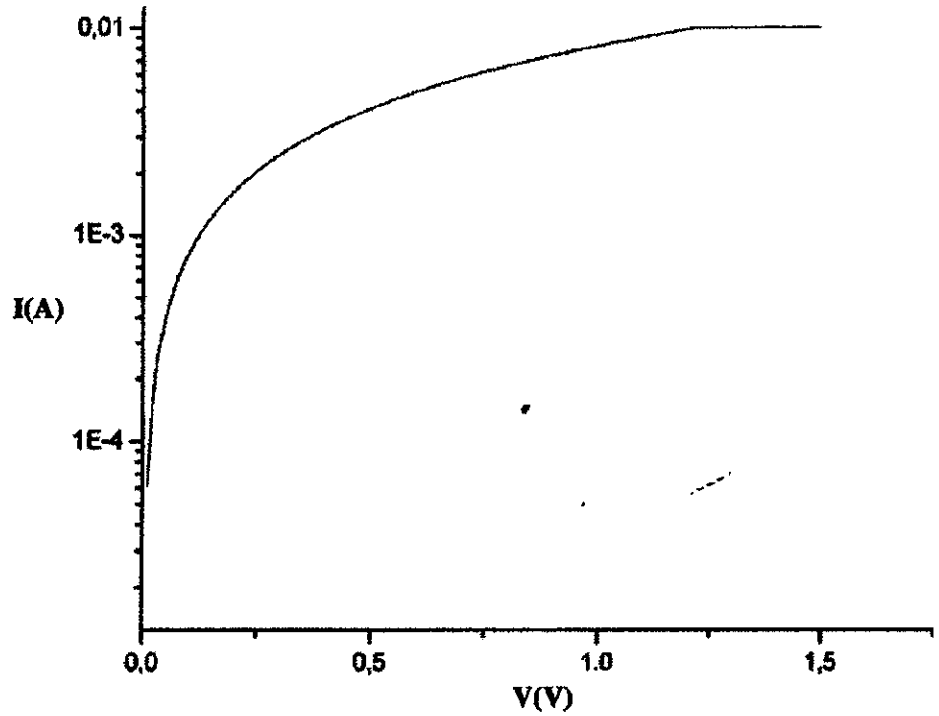

Figure 7. I-V curve of the sample with gold implanted dose of 1.15 x 10^{16} atoms/cm^2 on PMMA. It shows that the material is a semiconductor.

Summary and Conclusion

In this work we described a new semiconductor material made by PMMA doped with gold using very low energy ion implantation. In addition, nanolithography was performed on the PMMA generating an anisotropic surface morphology, resulting in an anisotropic resistivity. Samples with different geometries were prepared: one of them was fabricated with parallel lines along the substrate length and the second one with parallel lines perpendicular to it. The PMMA with gold implanted presented resistivities in the range 7.7 x 10^{-8} $\Omega.m$ to 0.23 $\Omega.m$. For any PMMA surface morphology the resistivity decreased when the gold dose increased.

It was expected that the sample with lithographed lines parallel to the direction of the substrate length should have lower resistivity than the sample with lithographed lines parallel to the direction perpendicular to the substrate length. But the result was just the opposite. To interpret this result, we analyzed the lithography process, showing that the morphological wavelength (λ) observed by AFM images of the PMMA nanolithographed is not small enough do produce the resistivity anisotropic effect. Following we suggested a possible justification for the observed resistivity anisotropy, based on a preferential orientation of the PMMA main-chains produced by the AFM nanolithography. This interpretation can justify the lower sample resistivity for the lithographed lines along the perpendicular direction of the substrate length.

The anisotropic factor for both morphologies described above presented a prominent peak for a dose of 1.15 x 10^{16} atoms/cm^2. With higher doses (> 2 x 10^{16} atoms/cm^2), we suggest that the preferential orientation of the main-chains was progressively destroyed during the gold implantation, consequently, reducing the anisotropic effect as observed.

Finally, a new sample of PMMA with gold implanted dose of 1.15 x 10^{16} atoms/cm^2 was prepared and an I-V curve was obtained, showing clearly that the material is a semiconductor.

Acknowledgments

The authors are grateful to FAPESP and CNPq for financial support.

References

1. R.E. Prange and Tsu-Wei Nee, *Phys.Rev.***168**, 779 (1968).
2. G.Fischer and H.Hoffmann, *Z.Physik-Condensed Matter* **39**, 287 (1980).
3. S. Mori and T. Ando, *J. Phys. Soc. Jpn.* **48**, 865 (1980).
4. T. Ando, A.B. Fowler and F. Stern, *Rev. Mod. Phys.* **54**, 437 (1982).
5. Z. Tesanovic, M.V. Jaric, S. Maekawa, *Phys. Rev. Lett.* **57**, 2760 (1986).
6. H. Sasaki, T. Noda, K. Hirakawa, M. Tanaka and T.Matsusue, *Appl. Phys. Lett.* **51**, 1934 (1987).
7. G. Fishman, D. Calecki, *Phys. Rev. Lett.* **62**, 1302 (1989).
8. G. Fishman, D. Calecki, *Phys. Rev.* **B43**, 11581 (1991).
9. G. Palasantzas, J. Barnas, *Phys. Rev.* **E56**, 7726 (1997).
10. G. Palasantzas, *Phys. Rev.* **B58**, 9685 (1998).
11. M.C. Salvadori, A.R.Vaz, R.C.Farias and M. Cattani, *Surf. Rev. Lett* **11**, 223 (2004).
12. M.Cattani and M.C. Salvadori, *Surf. Rev. Lett.* **11**, 283 (2004).
13. M.Cattani and M.C. Salvadori, *Surf. Rev. Lett.* **11**, 463 (2004).
14. M.C. Salvadori, L.L. Melo, A.R. Vaz, R.S. Wiederkehr, F. S. Teixeira and M. Cattani, *Surf. Coat. Technol.* **200**, 2965 (2006).
15. M.Cattani, M.C. Salvadori, F.S. Teixeira, R.S. Wiederkehr and I.G. Brown - "Electrical resistivity of very thin metallic films with isotropic and anisotropic surface". Accepted for publication in *Surf. Rev. Lett.*
16. M.C. Salvadori, M. Cattani, F.S. Teixeira, R.S. Wiederkehr and I.G. Brown, *J. Vac. Sci. Technol. A* **25**, 330 (2007).
17. M.C. Salvadori, I.G. Brown, A.R. Vaz, L.L. Melo and M. Cattani, *Phys. Rev. B* **67**, 153404 (2003).
18. D.R. Martins, M.C. Salvadori, P. Verdonk, I.G.Brown, *App. Phys. Let.* **81**, 1969 (2002).
19. A. Anders, G.Y.Yushkov, *J. Appl. Phys.* **91**, 8 (2002).
20. Website *SRIM (Stopping and Range of Ions in Matter)*, <http://www.srim.org> 2007.
21. I.G. Brown, "Cathodic Arc Deposition of Films", in *Annual Review of Materials Science*, Vol. 28 (Annual Reviews, Inc., Palo Alto, CA, 1998).
22. W.K. Pratt, *Digital Image Processing*: PIKS, 3rd Edition, Wiley, New York, (2001).
23. E.A. Dobisz, S.L. Brandow, E. Snow and R. Bass, *J. Vac. Sci. Tech.* **B 15**, 2318 (1997).
24. E.A. Dobisz, S.L. Brandow, R. Bass, and L.M. Shirey, *J. Vac. Sci. Tech.* **B 16**, 3695 (1998).
25. J. S. Ha, H. Roh, S. Jung, S. Park, J. Kim, E. Lee, *J. Vac. Sci. Technol.* **B 12**, 1977 (1994).

26. Y. Shao, S. A. Solin, D. R. Hines, E.D. Williams, *J. Appl. Phys.* **100**, 044512-1 (2006).
27. T.R. Albrecht, M.M. Doveck, C.A. Lang, P. Grütter, C.F. Quate, S.W.J. Kuan, C.W.Frank, R.F.W. Pease, *J. Appl. Phys.* **64**, 1178 (1986).
28. A. C. Genix, A. Arbe, F. Alvarez, J. Colmenero, W. Schweika, D. Richter, *Macromolecules* **39**, 3947 (2006).